

Silicon–hydroxyapatite bioactive coatings (Si–HA) from diatomaceous earth and silica. Study of adhesion and proliferation of osteoblast-like cells

M. López-Álvarez · E. L. Solla · P. González ·
J. Serra · B. León · A. P. Marques ·
R. L. Reis

Received: 7 October 2008 / Accepted: 1 December 2008 / Published online: 13 December 2008
© Springer Science+Business Media, LLC 2008

Abstract The aim of this study consisted on investigating the influence of silicon substituted hydroxyapatite (Si–HA) coatings over the human osteoblast-like cell line (SaOS-2) behaviour. Diatomaceous earth and silica, together with commercial hydroxyapatite were respectively the silicon and HA sources used to produce the Si–HA coatings. HA coatings with 0 wt% of silicon were used as control of the experiment. Pulsed laser deposition (PLD) was the selected technique to deposit the coatings. The Si–HA thin films were characterized by Fourier Transformed Infrared Spectroscopy (FTIR) demonstrating the efficient transfer of Si to the HA structure. The *in vitro* cell culture was established to assess the cell attachment, proliferation and osteoblastic activity respectively by, Scanning Electron Microscopy (SEM), DNA and alkaline phosphatase (ALP) quantification. The SEM analysis demonstrated a similar adhesion behaviour of the cells on the tested materials and the maintenance of the typical osteoblastic morphology along the time of culture. The Si–HA coatings did not evidence any type of cytotoxic behaviour when compared with HA coatings. Moreover, both the proliferation rate and osteoblastic activity results showed a slightly better

performance on the Si–HA coatings from diatoms than on the Si–HA from silica.

1 Introduction

A new generation of bioactive coatings has emerged with the silicon substituted hydroxyapatite thin films (Si–HA). This hydroxyapatite, modified with the inclusion of small concentrations of silicon has been demonstrating to improve the osteoblast proliferation and the bone extracellular matrix production [1]. The important role of silicon for skeletal and connective tissue development, especially in the early stage of bone formation, was first supported by Carlisle [2], who concluded that chicks fed with very low silicon content on diets showed reduced average mass, deformities in the comb and skin, and a retarded skeletal development noticed in the end of bones like tibia, femur and metatarsus. A recent study that consisted in the comparison of dietary silicon intake with bone mineral density in humans concluded that the bone mineral density was positively and significantly linked to dietary Si intake in men and premenopausal women [3].

A recent theory has asserted that the benefits occur because the Si–HA coatings would release low quantities of silicon and calcium ions, stimulating the activation of seven families of genes in osteoblasts, and consequently increasing osteoblast proliferation and differentiation [1]. Moreover, Si substitution is assumed to increase the solubility, to generate a more electronegative surface and to create a thinner microstructure resulting in a transformation of the implant surface into a more biologically equivalent apatite [3].

Other studies [4–6], have demonstrated that the presence of high levels of released silicon ions from the coating

M. López-Álvarez (✉) · E. L. Solla · P. González · J. Serra ·
B. León

Department of Applied Physics, E.T.S.I. Industriales, University
of Vigo, Campus Lagoas-Marcosende, 36310 Vigo, Spain
e-mail: miriammsd@uvigo.es

A. P. Marques · R. L. Reis
3B's Research Group—Biomaterials, Biodegradables and
Biomimetics, Department of Polymer Engineering, University
of Minho, Campus de Gualtar, 4710-057 Braga, Portugal

A. P. Marques · R. L. Reis
IBB—Institute for Biotechnology and Bioengineering,
Braga, Portugal

could contribute to extracellular pH changes, causing the alteration of the potential across the cell membrane and cell apoptosis. Cells, including osteoblasts, are sensitive to these possible changes in pH, an issue to consider when designing osteoinductive biomaterials. Thus, it is important to take into account the silicon content in the coating, since that, the content found in mineral bone ranges from trace levels of 0.1 to 0.5 wt% at the earliest stages of calcification [3]. It is also desirable the production of silicon containing apatites without secondary phases or additional substitution of ionic groups (apart of silicon) because they have made difficult in some experiments to determine the true role of silicon [7].

Silica (silicon dioxide, SiO₂) can be obtained synthetically and, also, it is commonly found in nature from lithogenic sources as in silica-rich rocks such as obsidian, granite, diorite, and sandstone. The most significant silicate minerals are feldspar and quartz; in fact, the most pure sand is quartz (silica). In respect to the biogenic sources, the diatomaceous earth constitutes the largest source of biogenic amorphous silica and the most abundant form of silica on earth. It consists of the mineralised exo-skeletons of diatoms, which are unicellular algae encased by a silicious cell wall, termed frustules. The constant “rain” of dead diatom frustules to the bottom of the ocean results in the accumulation in large fossil deposits of amorphous polymerized silicic acid. This biogenic source has a great potential because of its abundance and an inexpensive cost [8–10].

Within the all available techniques to produce the Si–HA coatings, the pulsed laser deposition (PLD) technique is very promising to obtain high quality coatings. This technique offers unique features as the absence of contamination because of the use of laser light under vacuum conditions. Moreover, it allows the growth of materials with high melting point and a good control of the coatings stoichiometry [11–13].

In this study we have investigated the suitability of the Si–HA coatings to support the attachment, proliferation and osteogenic activity of the osteoblast-like cells SaOS-2. A comparative study of the Si–HA coatings obtained from two different sources of silicon (diatomaceous earth and silica) is also discussed.

2 Materials and methods

2.1 Si–HA bioactive coatings

Titanium discs (5 mm of diameter and 1 mm of thickness) were coated by Si–HA coatings. The experimental system was an ArF excimer laser (193 nm), operating at 200 mJ and a pulse repetition rate of 10 Hz which irradiates the

ablation target described elsewhere [11, 12]. Two types of targets were prepared from mixtures of commercially available carbonated HA (Plasma Biotal, Captal1 R) and two different sources of silicon: diatomaceous earth (92.3 wt% SiO₂, 3.6 wt% Fe and 1.5 wt% Al, Mg, Ca, P, K and Na) and pure silica (99.5 wt% SiO₂).

Films were deposited in a low pressure water vapour atmosphere (0.45 mbar) to improve the quality of the coatings, and the Ti substrates were maintained at 460°C during the film growth. Films were grown during 3.5 h of deposition time which yields a coating with an approximate thickness of 7 µm. Titanium discs with HA coatings (0% of Si) were also analyzed.

The thin film properties were evaluated through the IR active groups by Fourier Transformed Infrared spectroscopy (FTIR) with a Bruker IFS28 spectrometer.

To the osteoblast-like cells assay, the materials were sterilized by gamma radiation.

2.2 Cell study

The biological performance of the developed ceramic coatings was assessed in a direct contact assay with a human osteoblast-like cell line (SaOS-2). The selection of these human osteoblasts came favoured because of their ability to synthesize most of the proteins present in the extracellular matrix (ECM) and to control its mineralization. Thus they regulate the ingrowth of bone to the implant [14–19].

Samples were placed in 48-well plates and 1 ml of a cell suspension of SaOS-2 in Dulbecco's Modified Eagle Medium (DMEM; Sigma, USA), supplemented with 10% Foetal Bovine Serum (FBS; Invitrogen, USA) and 1% of antibiotic/antimycotic solution (A/B Invitrogen, USA) in a concentration of 3.3×10^4 cells/per ml was added in each well.

Cells were cultured on the ceramic coatings for 1, 3 and 7 days in a humidified atmosphere with 5% CO₂ and at 37°C. Medium was changed every 2–3 days. Three discs of each material were used per experiment. Tissue culture polystyrene (TCPS) was used as control of the assay.

2.3 Scanning electron microscopy analysis

Cell adhesion and morphology were analyzed by Scanning Electron Microscopy (SEM). After each incubation time the seeded discs were washed twice with Phosphate Buffer Saline (PBS; Sigma, USA) and fixed with 2.5% glutaraldehyde in 0.1 M PBS for 30 min at 4°C. Samples were washed again with PBS and dehydrated in graded ethanol solutions (50%, 70%, 90% and 100% v/v) twice for 15 min each concentration. The samples were maintained in 100% v/v ethanol until being subjected to hexamethyldisilazane

(HDMS; Electron Microscopy Science, USA) desiccation. The discs were finally mounted on metal stubs and sputter-coated with gold prior to their analysis using a Leica Cambridge S360 Scanning Electron Microscope.

2.4 dsDNA and ALP activity quantification

Cell proliferation was assessed by total dsDNA quantification along the time of culture. The osteogenic activity was followed by determining the activity of alkaline phosphatase (ALP), a marker of early osteogenic differentiation, throughout the different incubation times. Discs were carefully rinsed twice with PBS and immersed in water. Thus, cell lysates were obtained after the osmotic shock followed by a thermal shock by transferring the lysates from 37 to -80°C .

The dsDNA content of each sample was measured using the lysates and the PicoGreen dsDNA Quantification Kit (Molecular Probes) following manufacturer instructions. Fluorescence was read in a microplate reader (Bio-Tek, USA) at 485 ex/525 em.

The same cell lysates were used to quantify the activity of ALP. ALP activity was measured using a *p*-nitrophenol assay. Briefly, *p*-nitrophenyl phosphate, which is colorless, is hydrolysed by alkaline phosphatase at pH 10.5 and 37°C to form free *p*-nitrophenol, which is yellow. The reaction was stopped by adding NaOH and the absorbance read at 405 nm in a microplate reader (Bio-Tek, USA). The ALP activity values were normalized against the amount of dsDNA.

2.5 Statistical analysis

Data are presented as mean \pm standard deviation ($n = 3$). Error bars in figures represent standard deviations. Differences between groups were analyzed according to a Student's *t*-test with $P < 0.05$ considered statistically significant.

3 Results

3.1 Properties of the Si–HA coatings

In previous works [11, 12], a systematic study on the properties of Si–HA coatings produced by PLD with different proportions has been reported. The Si–HA films were derived from two different targets using a mixture of commercial carbonated HA, which presents more resemblance with the biological apatite because of the presence of carbonate ions, and either diatomaceous earth or pure silica as source of silicon. Taking into account the literature we have selected Si–HA coatings with high content of

silicon to check their potential to support osteoblast cells in extreme conditions. Figure 1 summarizes the main results on the bonding configuration of Si–HA coatings with 7.5 wt% of Si for both approaches (diatomaceous earth and silica sources). HA coating has been used as control.

The Fourier Transform Infrared Spectroscopy (FTIR) spectrum of the HA coating (Fig. 1a) shows the main absorption bands corresponding to carbonated hydroxyapatite (A): (i) 1000–1200, 960 and 560 cm^{-1} , respectively, attributed to asymmetric stretching, symmetric stretching and asymmetric bending vibrations of PO_4^{3-} groups, (ii) the 1400–1500 and 875 cm^{-1} that are assigned to asymmetric stretching and bending vibration of CO_3^{2-} groups, respectively. The absorption observed at 3575 cm^{-1} corresponds to the stretching vibration of the OH groups that are present in the HA structure.

The comparison of the absorption patterns of the different coatings revealed many differences while the introduction of Si is carried out. If we take the HA sample (0 wt% Si) as the reference material (Fig. 1a), there is an evident diminution of the intensities of the CO_3^{2-} absorptions as the silicon is incorporated in both series (Fig. 1b, c). In addition as the silicon source concentration increases on the targets, the spectrum broadens, which can be attributed to a decrease of the degree of crystallinity when silicon is incorporated [11, 12]. This loss of crystallinity is more intense at the Si–HA diatomaceous coating compared to the silica if we attend the 1000–1200 cm^{-1} absorption band attributed to asymmetric stretching of PO_4^{3-} and also at the 560 cm^{-1} with a lower absorbance intensities and wider spectrum broadens.

As it can be observed in the FTIR results the structure and chemical composition characterization has proved the efficient incorporation of Si to the HA structure in the form of

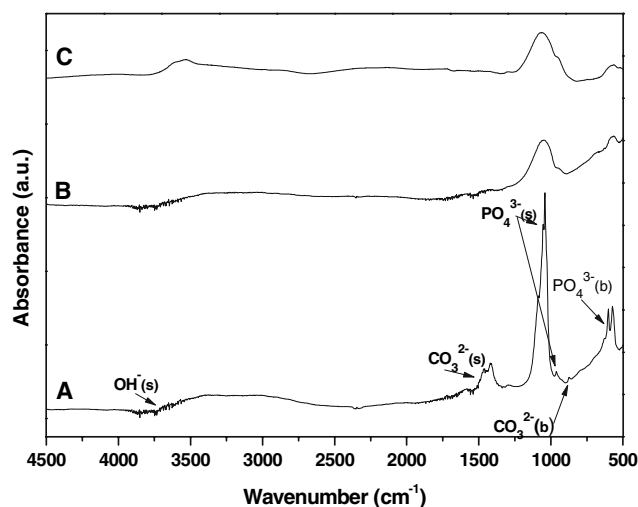


Fig. 1 FTIR spectra for HA coating (a), Si–HA silica coating (b) and Si–HA diatom coating (c)

SiO_4^{4-} groups. Several differences between the two Si–HA coatings spectra were identified indicating a slight but clear improved incorporation of Si into the Si–HA diatomaceous coating in comparison to the Si–HA silica one.

3.2 Cell morphology

SEM analysis was performed to evaluate the morphology of cells grown on the two different Si–HA coatings along the time of culture (1, 3 and 7 days). In Fig. 2 the most representative images are shown.

The SEM micrographs demonstrated the absence of cytotoxicity of the Si–HA coatings in direct contact with osteoblasts-like cells SaOS-2 up to 7 days of culture.

The comparison of the morphologies of the osteoblast-like cells on the studied surfaces revealed similar results along the time of culture. Cells attached and spread well on the coatings, maintaining their typical polygonal morphology although at early time points cells displayed a more flatten morphology on HA and Si–HA from diatoms. This effect was softened for longer culture times, which allowed us to conclude that the effect of the Si–HA

coatings, over cell morphology, did not differ from the observed on the HA coating.

3.3 Cell proliferation

Cell proliferation on the tested coatings is represented in Fig. 3 as the variation of the DNA amount of the cells adhered to both of the different coatings and to the controls, along the time of culture. The DNA measurements showed a continuous cell growth from day 1 to day 7 on the tested coatings and also in the control samples although at

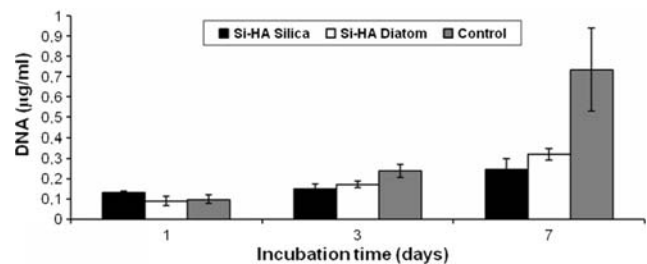
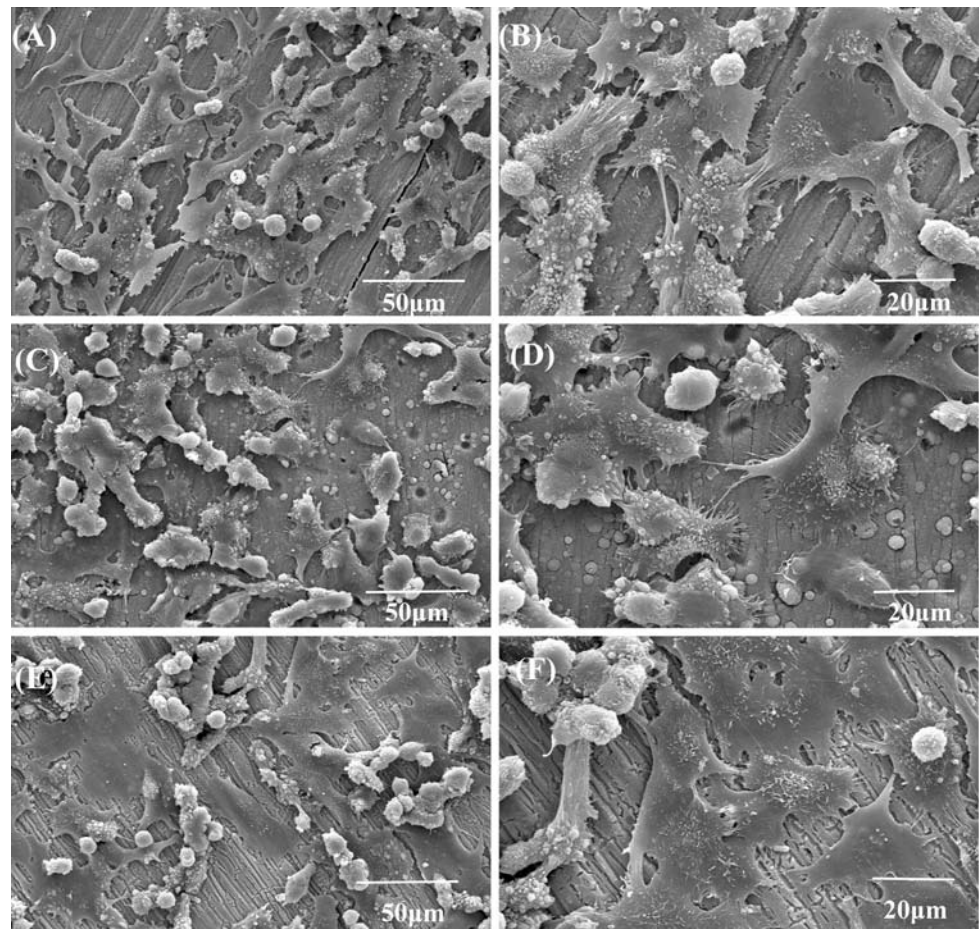


Fig. 3 dsDNA quantification results presented in µg/ml of osteoblastic-like cells (SaOS-2) cultured on Si–HA coatings up to 7 days

Fig. 2 SEM micrographs of osteoblast-like cells cultured up to 7 days on HA coating, **a** (×500) and **b** (×1000), Si–HA coating from silica, **c** (×500) and **d** (×1000) and Si–HA coating from diatomaceous earth, **e** (×500) and **f** (×1000)



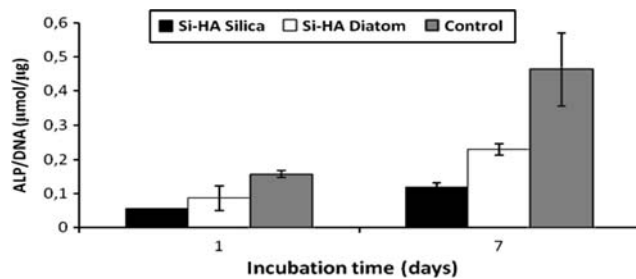


Fig. 4 ALP activity quantification results presented in pNP hydrolyzed/cell, of osteoblastic-like cells (SaOS-2) cultured on Si–HA coatings up to 7 days

different rates. The comparison between the two different Si–HA coatings showed a slightly higher proliferation on the Si–HA coatings from diatoms from day 3 to day 7 (significant difference on day 7, $P < 0.05$) than on to the Si–HA coating from silica. The proliferation was significantly higher ($P < 0.05$) on the control than to the both Si–HA coatings and indicates the healthy stage of the cells.

3.4 Osteoblastic activity

The ALP results were normalized against the dsDNA values obtained for the same samples, as previously described. Figure 4 indicates the ALP activity evolution from day 1 to day 7 of culture. The ALP activity per cell increased in all the tested coatings from 1 to 7 days. The highest values of ALP activity corresponded to the control sample at day 7. Although during the first day of cell culture there were no significant differences ($P < 0.05$) in the osteoblastic activity between both Si–HA coatings, at the 7 day the ALP activity values for the cells adhered to the Si–HA from diatomaceous earth was significant higher ($P < 0.01$) than to the Si–HA from silica.

It is important to stress that all the mean values along the experiment were, in respect to the silica, higher at the Si–HA diatomaceous coating. This higher osteoblastic activity at the diatomaceous coating can be probably explained by the presence of the minority elements at the coating composition. As previously reported [12], in Table 1 it is shown the analysis by the Ion Beam technique of the ion traces of the HA coating and the two Si–HA coatings. The results showed a higher content of minority compounds as Na, Mg, Al, K

Table 1 Composition of the HA and Si–HA coatings measured by Ion Beam Technique (from Ref. [12])

Series	Si target (at.%)	Na (at.%)	Mg (at.%)	Al (at.%)	K (at.%)	Fe (at.%)
HA	0	0.02	0.2	0.08	0.02	0.02
Si–HA silica	7.5	0.02	0.2	0.1	0	0
Si–HA Diatom	7.5	0.09	0.3	0.5	0.06	0.02

and Fe at the Si–HA coating from diatomaceous earth than on the Si–HA from silica. Therefore, the Si–HA coatings from diatomaceous earth presented a composition more similar to the HA found in the bone what could have favoured a better biological performance.

It is already proved that silicon improves the osteoblastic proliferation and the bone extracellular matrix production because of the stimulation of specific families of genes [1]. Recently it was demonstrated, by Weichang Xue et al. [20], that the presence of strontium stimulates, as well, cell differentiation to osteoblast and it encourages the osteoblastic activity. It is well known that the biological HA is complemented by the presence, in trace levels, of other ions such as carbonate, magnesium, fluoride, silicon, strontium. Each one of these ions, by separate, can induce some beneficial effects, but, in our results we demonstrated that a mixture of different ions in trace quantities, also with silicon, promoted a better biological performance of the osteoblasts cells than with the unique addition of silicon.

4 Conclusions

The study of adhesion and proliferation of osteoblast-like cells has proved the absence of cytotoxicity of the Si–HA coatings from diatomaceous earth and silica tested. After 7 days of cell culture the results indicated that Si–HA coating from diatomaceous earth significantly favoured ($P < 0.01$) osteoblast proliferation and activity in comparison to the Si–HA coating from silica.

Acknowledgments This work was supported by the UE-Interreg IIIA (SP1.P151/03) Proteus project and Xunta de Galicia (Projects: 2006/12 and PGIDITO5PXIC30301PN).

References

- L.L. Hench, J.R. Jones, *Biomaterials, Artificial Organs and Tissue Engineering* (Woodhead Publishing in Materials, Cambridge, 2005)
- E.M. Carlisle, *J. Nutr.* **110**(5), 1046–1055 (1980)
- A.M. Pietak, J.W. Reid, M.J. Stott, M. Sayer, *Biomaterials* **28**(28), 4023–4032 (2007). doi:10.1016/j.biomaterials.2007.05.003
- J.E. Gough, J.R. Jones, L.L. Hench, *Biomaterials* **25**(11), 2039–2046 (2004). doi:10.1016/j.biomaterials.2003.07.001
- E.S. Thian, J. Huang, S.M. Best, Z.H. Barber, W. Bonfield, *Mater. Eng. C* **27**(2), 251–256 (2006). doi:10.1016/j.msec.2006.05.016
- E.S. Thian, J. Huang, M.E. Vickers, S.M. Best, Z.H. Barber, W. Bonfield, *J. Mater. Sci.* **41**(3), 709–717 (2006). doi:10.1007/s10853-006-6489-8
- N. Patel, S.M. Best, W. Bonfield, *J. Mater. Sci-Mater. M* **13**(12), 1199–1206 (2002). doi:10.1023/A:1021114710076
- C. Van Den Hoek, D.G. Mann, H.M. Jahns, *Algae: An Introduction to Phycology* (Cambridge University Press, Cambridge, 1995)

9. Z. Elias, O. Poirot, I. Fenoglio, M. Ghiazza, M.C. Danieri, F. Terzetti, C. Dame, C. Coulais, I. Matekovits, B. Fubini, *Toxicol. Sci.* **91**(2), 510–520 (2006). doi:[10.1093/toxsci/kfj177](https://doi.org/10.1093/toxsci/kfj177)
10. S.M. Holmel, B.E. Graniel-Garcia, P. Foran, P. Hill, E.P.L. Roberts, B.H. Sakakini, J.M. Newton, *Chem. Commun. Camb.* **25**, 2662–2663 (2006). doi:[10.1039/b600708b](https://doi.org/10.1039/b600708b)
11. E.L. Solla, J.P. Borrajo, P. González, J. Serra, S. Chiussi, B. León, J. García López, *Appl. Surf. Sci.* **253**(19), 8282–8286 (2007). doi:[10.1016/j.apsusc.2007.02.116](https://doi.org/10.1016/j.apsusc.2007.02.116)
12. E.L. Solla, P. González, J. Serra, S. Chiussi, B. León, J. García López, *Appl. Surf. Sci.* **254**(4), 1189–1193 (2007). doi:[10.1016/j.apsusc.2007.09.041](https://doi.org/10.1016/j.apsusc.2007.09.041)
13. A. Bigi, B. Bracci, F. Cuisinier, R. Elkaim, M. Fini, I. Mayer, I.N. Mihailescu, G. Socol, L. Sturba, P. Torricelli, *Biomaterials* **26**(15), 2381–2389 (2005). doi:[10.1016/j.biomaterials.2004.07.057](https://doi.org/10.1016/j.biomaterials.2004.07.057)
14. L.C. Baxter, V. Frauchigen, M. Textor, I. Ap Gwynns, R.G. Richards, *Eur. Cell. Mater.* **4**, 1–17 (2002)
15. H.H. Lu, S.F. El-Amin, K.D. Scott, C.T. Laurencin, J. Biomed. Mater. Res. Part A **64**(3), 465–474 (2003). doi:[10.1002/jbm.a.10399](https://doi.org/10.1002/jbm.a.10399)
16. U. Mayr-Wohlfart, J. Fiedler, K.P. Günther, W. Puhl, S. Kessler, *J. Biomed. Mater. Res.* **57**, 132–139 (2001). doi:[10.1002/1097-4636\(200110\)57:1<132::AID-JBM1152>3.0.CO;2-K](https://doi.org/10.1002/1097-4636(200110)57:1<132::AID-JBM1152>3.0.CO;2-K)
17. M. Rouahi, O. Gallet, E. Champion, J. Dentzer, P. Hardouin, K. Anselme, *J. Biomed. Mater. Res. Part A* **78**, 222–235 (2006)
18. F. Causa, P.A. Netti, L. Ambrosio, G. Ciapetti, N. Baldini, S. Pagani, D. Martini, A. Giunti, *J. Biomed. Mater. Res. Part A* **76**, 151–162 (2006)
19. H.C. Schroder, O. Boreiko, A. Krasko, A. Reiber, H. Schwertner, W.E.G. Muller, *J. Biomed. Mater. Res. Part B* **75**(2), 387–392 (2005). (Appl. Biomater.)
20. W. Xue, J.L. Moore, H.L. Hosick, S. Bose, A. Bandyopadhyay, W.W. Lu, K.M.C. Cheung, K.D.K. Luk, *J. Biomed. Mater. Res. Part A* **79**, 804–814 (2006)